IEEE Access
Multidisciplinary | Rapid Review | Open Access Journal

Received 16 May 2024, accepted 29 May 2024, date of publication 5 June 2024, date of current version 14 June 2024.

Digital Object Identifier 10.1109/ACCESS.2024.3409690

TOPICAL REVIEW

Applications of Wireless Power Transfer System in Motors: A Review

KE LI[1], YUANMENG LIU[1], XIAODONG SUN[2], (Senior Member, IEEE), XIANG TIAN[2], AND GANG LEI[3], (Senior Member, IEEE)

[1]School of Electrical and Information Engineering, Jiangsu University, Zhenjiang 212013, China
[2]Automotive Engineering Research Institute, Jiangsu University, Zhenjiang 212013, China
[3]School of Electrical and Data Engineering, University of Technology Sydney, Sydney, NSW 2007, Australia

Corresponding authors: Xiaodong Sun (xdsun@ujs.edu.cn) and Xiang Tian (auzn0009@163.com)

This work was supported by the National Natural Science Foundation of China under Project 5200120162.

ABSTRACT This article provides a comprehensive overview of on-board wireless motors based on WPT system. Based on the mathematical models of common wireless motors, the coupling strength of on-board wireless motors is divided, and their characteristics and advantages are comprehensively summarized and classified. In order to provide power to the three-phase wireless motors, the rotary transformer is used to replace the common coupling coil in the WPT system. This paper conducts electromagnetic model on the rotary transformer, as well as a comprehensive summary of structures and materials of the rotary transformer. The resonant compensation topology of WPT system is crucial. Comparing the transmission characteristics and advantages and disadvantages of various compensation topologies is beneficial for selecting appropriate compensation topologies in different application scenarios. For the control strategy of WPT system, this paper mainly focuses on the issues of output power and transmission efficiency. Finally, the research difficulties and directions of on-board wireless motors are proposed, such as electromagnetic interference and resonance, and this technology is extended to other fields, including wireless charging, robotics, etc.

INDEX TERMS Wireless power transfer (WPT), wireless motor, couplers, compensation topologies, control strategies, electromagnetic interference (EMI), resonance, wireless charging.

I. INTRODUCTION

Petroleum is one of the most crucial energy resources globally, extensively utilized in transportation, industrial production, and chemical manufacturing. However, vehicles emit significant amounts of greenhouse gases, such as carbon dioxide, during operation, thereby exacerbating global warming and climate change [1]. In response to this pressing environmental concern, new energy vehicles have emerged [2], including electric vehicles, hybrid vehicles, and hydrogen fuel electric vehicles [3]. The central component of these new energy vehicles is the onboard motor. Presently, the most prevalent onboard motors in the market include permanent magnet synchronous motors (PMSMs) [4], [5], electrically excited synchronous motors (EESMs), switched reluctance motors (SRMs) [6], [7], axial-flux motors [8], [9]. Among these motors, PMSMs dominate the automotive market due to wide speed range, high torque density, high power density, and low maintenance cost [10], [11]. PMSMs generate magnetic fields internally through permanent magnets [12], and the magnetic field of PMSMs remains fixed, which makes it difficult to adjust the strength and position of the magnetic field. SRMs are known for their high starting torque, lack of permanent magnets, and independence of phases, which contribute to their high efficiency. However, the inherently doubly salient structure of SRMs leads to highly nonlinear magnetic and torque characteristics, which poses challenges for their control strategies [13], [14]. EESMs generate magnetic fields via external excitation currents, and the motor allows for speed regulation through adjustment of the excitation current [15], [16].

For new energy vehicles, the battery serves as the driving power source for the on-board motor. The progress of on-board motor and drive technology should be combined

The associate editor coordinating the review of this manuscript and approving it for publication was Wei Xu.

with advanced technologies. In recent years, wireless power transmission (WPT), lightweight design, and compact system integration design have emerged, all of which aim to minimum the volume and weight of system. For on-board motors, using a WPT system for power supply can save some coils and inverters, reduce the size and weight, thereby improving the operational quality. The concept of wireless motors originated from the University of Tokyo [32], where the research team proposed a wireless motor used for wheel motors in electric vehicles.

Through WPT system, the electrical energy in the battery is transmitted to the on-board motor, which in turn drives the operation of the motor and vehicle (as shown in Figure 1). WPT system has developed many years and is widely used in electric vehicle charging [33], [34], biomedical medical [35], [36], radio-frequency [37], [38] and other fields. Table 1 lists the on-board wireless motors and provides a detailed description of their characteristics and advantages. According to the different coupled degrees and motor characteristics, wireless motors can be divided into three types: weakly-coupled wireless motors, mid-coupled wireless motors, and strongly-coupled wireless motors.

1) Weakly coupled wireless motor: The receiving side of the WPT system requires a rectifier and inverter. These components are necessary to convert the high-frequency energy received from the transmitter to low-frequency energy suitable for the motor. Additionally, in order to control the operation of the wireless motor, the control signal needs to be transmitted to the receiving side through additional communication circuits.

2) Mid-coupled wireless motor: some power electronic components can be eliminated from the receiver side. However, certain rectifiers and inverters are still retained. The control signal can be mixed within the power flow and transmitted to the receiving side, enabling control of the wireless motor. In certain well-designed motors, the receiving side may not require any control signals and operates autonomously based on the power flow.

3) Strongly-coupled wireless motor: No need for a conversion circuit inside the receiver side. Instead, the transmitter controls the energy amplitude and frequency according to the motor's requirements. This allows for precise control and efficient power transfer. In some well-designed motors, a portion of the stator coil can also serve as a receiving coil, further optimizing the efficiency of the wireless motor.

In order to apply the WPT system to the motor, the ordinary coupling coil of the WPT system can no longer meet the requirements. Therefore, the rotary transformer is used to replace the coupling coil to achieve power supply for the three-phase motor. This article presents an electromagnetic modeling of the rotary transformer and provides a comprehensive study and summary of its structure and materials. This will help researchers explore simpler and better transmission performance rotary transformers based on previous research. In addition, the resonant compensation topologies directly affect the transmission performance of WPT systems, and different topology structures have different transmission effects and advantages and disadvantages. Therefore, a comprehensive induction and summary of the resonant compensation topology and control strategy of the WPT system have also been conducted. Finally, in view of the fact that on-board wireless motors are in their early stages, there are numerous research difficulties and directions. Therefore, this article also puts forward opinions on this and summarizes the applications of motors in other fields.

The remaining parts of the paper are as follows: Section II design mathematical models for common wireless motors. Section III evaluates and summarizes the advanced research on the shape, material, and other aspects of the rotary transformer for on-board motors; Section IV summarizes and evaluates the resonant compensation topologies of the WPT system; Section V summarizes the control strategies of the WPT system, which includes stabilizing transmission power and improving transmission efficiency. Section VI analyzes some drawbacks and research directions of the on-board motors, and extends this technology to other application scenarios.

II. MATHEMATICAL MODELS OF WIRELESS MOTORS BASED ON WPT SYSTEM

When the WPT system is applied to different types of motors, its mathematical model is related to the operational quality of the motor. This section conducts mathematical model analysis on common PMSM, IM, EESM and SRM.

A. PMSM BASED ON WPT SYSTEM

Electromagnetic torque of PMSM can be obtained as:

$$T = \frac{3P}{4}\left(\lambda_{ds}^{r} i_{qs}^{r} - \lambda_{qs}^{r} i_{ds}^{r}\right) \tag{1}$$

The voltages for three-phase stators are expressed as:

$$\begin{cases} V_{as} = V_m \sin \omega t \\ V_{bs} = V_m \sin\left(\omega t - 2\pi/3\right) \\ V_{as} = V_m \sin\left(\omega t - 2\pi/3\right) \end{cases} \tag{2}$$

where V_{as}, V_{bs}, and V_{cs} are voltages of stator phase; V_m are peak voltage of stator; ω are synchronous speed.

Converting the stator voltages in *abc* axis to the *dq* axes:

$$V_{qdo} V_{qdos} = K_s V_{abcs} \tag{3}$$

$$\begin{bmatrix} V_{ds} \\ V_{qs} \\ V_{os} \end{bmatrix} = \frac{2}{3} \begin{bmatrix} \cos\theta & \cos\left(\theta - 2\pi/3\right) & \cos\left(\theta + 2\pi/3\right) \\ \sin\theta & \sin\left(\theta - 2\pi/3\right) & \sin\left(\theta + 2\pi/3\right) \\ 1/2 & 1/2 & 1/2 \end{bmatrix} \times \begin{bmatrix} V_{as} \\ V_{bs} \\ V_{cs} \end{bmatrix} \tag{4}$$

Equation (4) describe the stator current in the synchronously rotating reference axes:

$$\begin{cases} i_{qs}^{e} = \int \dfrac{V_{qs}^{e}}{L_q} - \omega_e \dfrac{\lambda_{af}}{L_q} - \dfrac{R_s}{L_q} i_{qs}^{e} - \omega_e i_{ds}^{e} \dfrac{L_d}{L_q} \\ i_{ds}^{e} = \int \dfrac{V_{ds}^{e}}{L_d} - \dfrac{R_s}{L_q} i_{ds}^{e} - \omega_e i_{qs}^{e} \dfrac{L_q}{L_d} \end{cases} \tag{5}$$

TABLE 1. Wireless motors based on wireless power transfer.

Wireless motors	Features	Advantages
Direct current motor (DCM) [17-19]	1. DC motor drives WPT system to provide power. 2. Connecting multiple DC motors to the receiving circuit of WPT system, and controlling different types of motors by configuring the parameters of each receiving circuit. 3. Applying Non-Hermitian parity-time (PT) symmetry to enhance the performance of WPT system.	1. DC motor and WPT system can drive each other and operate independently. 2. WPT system can simultaneously supply power to multiple DC motors of different models, enabling one-to-many power transmission. 3. WPT system can ensure the steady-state operation of DC motors.
Permanent magnet synchronous motors (PMSM) [20, 21]	1. WPT system adopts L2CL-LCL topology for PMSM operation. 2. The three-phase rotor of the PMSM is directly powered by three individual transmission circuits of WPT system.	1.Through L2CL-LCL topology, the input power and efficiency of the PMSM increased. 2. Power electronics for WPT system is saved, enhancing its resistance to interference at operating frequencies.
Switched reluctance motor (SRM)[22, 23]	1. The utilization of Bluetooth for implementing WPT in SRMs entails periodic maintenance drawbacks. Substituting Bluetooth with a variable reluctance (VR) resolver mitigates these issues. 2. WPT system employs laminated magnetic couplers and utilizes commutative-resonant control to independently excite the coupling coils.	1.1. The VR resolver can circumvent the latency associated with Bluetooth, achieving phase synchronization between both ends of WPT system. 2.1 LMC not only enables power selectivity but also distance scalability. CRC can individually excite the corresponding coils within LMC, energizing the target phase windings of SRM.
Electrically excited synchronous motor (EESM)[16, 24, 25]	1. Does not require the converters and utilizes the variable carrier phase shift method to maintain constant input excitation voltage. 2. Modeling and parameter analysis of the EESM rotating transformer. 3. A reduced-order model based on local linear approximation of resonance voltage/current can reduces the 13th-order model to a 9th-order model of EESM.	1. Excitation current can remain constant under different motor drives, and adjusting the switching frequency can reduce the magnetic field current. 2. Optimal design parameters for the rotating transformer can be determined. 3. Enhancing the accuracy of the model in both the time and frequency domains.
Induction motor (IM)[26, 27]	1. IM brushless excitation system employs two resonant circuits, two full-bridge rectifiers, comparators, and two gate drivers. 2. A controllable speed is employed to drive the rotating transformer and power the auxiliary rotor, and the fundamental component of the air-gap magnetic field is responsible for torque generation.	1. Avoiding excessive transformers and diodes, simplifying the excitation system, and enabling stable control of speed and power aspects of IM. 2. Enabling effective decoupling control between torque and power.
In-wheel motor (IWM)[28, 29]	1. Analyzing the coupling coil structure of IWM. Investigating effect of mutual inductance and load variations on IWM. 2. Adding parallel super-capacitor and a bidirectional boost-buck converter to charge the super-capacitance during voltage reduction and discharge them during voltage boosting.	1. Determining the optimal structure for magnetic coupler (including coil material). 2. The super-capacitor enables the WPT system to maintain stable power transmission to the IWM.
Servo motor (SM) [30, 31]	1. Adopting a one-to-two transmission mode to directly control SM. 2. A microcontroller generates control signals to control circuits on receiving side. latch circuits and full-bridge circuits generate motor direction control signals.	1. The transmission mode ensures power balance between the two receiving coils, enabling bidirectional movement. 2. Achieving soft switching, power balance, and avoiding additional communication modules.

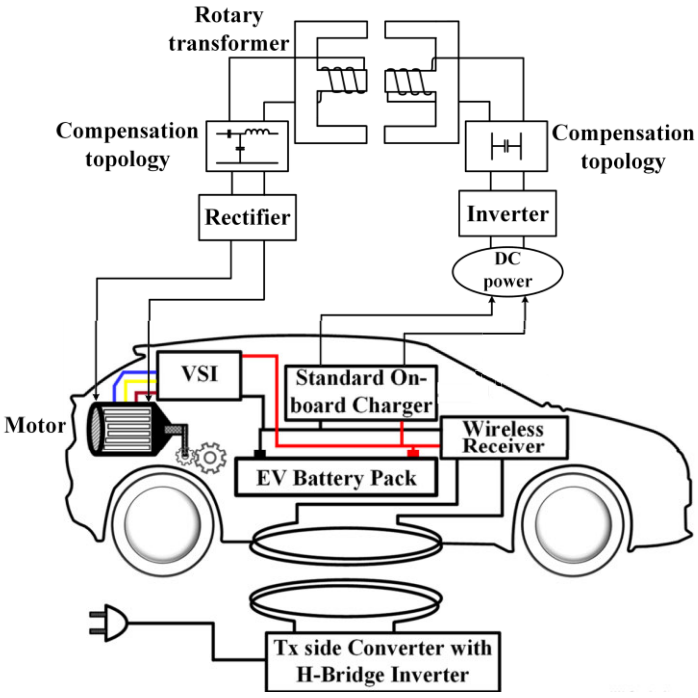

FIGURE 1. Structure diagram of wireless motor based on WPT.

where i^e_{ds} and i^e_{qs} represent the current at d axis and q axis; V^e_{ds} and V^e_{qs} represent the voltage at d axis and q axis.

The electromagnetic torque produced by the motor can be obtained as:

$$T = \frac{3P}{4}\left(\lambda_{af} i^e_{qs} + \left(L_d - L_q\right) i^e_{qs} i^e_{ds}\right) \tag{6}$$

The relationship between the load torque and electromagnetic torque are:

$$T_e = T_L + B\omega_m + J\frac{d\omega_m}{dt} \tag{7}$$

where P is the number of pole pairs; T_e is electromagnetic torque; T_L is Load torque; B is damping coefficient; J is moment of inertia; ω_m is rotor speed.

According to equation (), ω_m can be obtained as:

$$\omega_m = \frac{1}{J}\int T_e - T_L - B\omega_m \tag{8}$$

In addition, ω_m can bu used to describe the rotor angle θ_m.

Rotor electrical speed ω_e can be obtained as:

$$\omega_e = \frac{P}{2}\omega_m \tag{9}$$

B. IM BASED ON WPT SYSTEM

The rotating direct-quadrature axes transformed model of 3-phase IM can be described as:

$$\begin{cases} \dot{i}_{sd} = bp\Omega\Phi_{rq} + ba\Phi_{rd} - \gamma i_{sd} + \omega_s i_{sq} + m_1 u_{sd} \\ \dot{i}_{sq} = -bp\Omega\Phi_{rd} + ba\Phi_{rq} - \gamma i_{sq} - \omega_s i_{sd} + m_1 u_{sq} \\ \dot{\Phi}_{rd} = \left(\omega_s - p\Omega\right)\Phi_{rq} - a\Phi_{rd} + aM_{sr} i_{sd} \\ \dot{\Phi}_{rq} = -\left(\omega_s - p\Omega\right)\Phi_{rd} - a\Phi_{rq} + aM_{sr} i_{sq} \\ \dot{\Omega} = -c\Omega + m\left(\Phi_{rd} i_{sq} - \Phi_{rq} i_{sd}\right) - T_l/J \end{cases} \tag{10}$$

where i_{sd}, i_{sq} represent the stator current of d-axis and q-axis, Φ_{rd}, Φ_{rq} represent the stator flux of d-axis and q-axis, T_l represents load torque Ω is angular speed, ω_s is stator frequency and p is the number of pole-pair. γ can be described as follows:

$$\begin{cases} \gamma = \dfrac{L_r^2 R_s + M_{sr} R_r}{\mu L_s L_r^2} \\ \mu = 1 - \dfrac{M_{sr}^2}{L_s L_r} \end{cases} \tag{11}$$

where R_s and R_r are the resistances of stator and rotor, L_s and L_r are the inductances of stator and rotor, J is the inertia of motor and M_{sr} is mutual inductance between rotor and stator. $_{\mathrm{m}}$, m_1, a, b, c can be expressed as:

$$\begin{cases} m = pM_{sr}/(JL_r) \\ m_1 = 1/(\mu L_s) \\ a = R_r/L_r \\ b = M_{sr}/(\mu L_s L_r) \\ c = f_v/J \end{cases} \tag{12}$$

where f_v is coefficient of viscous damping.

The IM load current can be described as:

$$I_L = i_{sd} u_{sd} + i_{sq} u_{sq} \tag{13}$$

u_{sd}, u_{sq} are defined as follows based on input switch:

$$\begin{cases} u_{sd} = V_{out} u_d \\ u_{sq} = V_{out} u_q \end{cases} \tag{14}$$

where V_{out} is output voltage of WPT system, u_d and u_q are switching points of 3-phase inverter dq axis.

C. EESM BASED ON WPT SYSTEM

The current vector diagram of EESM is shown in Fig. 4. The dq-axis is transformed from stator current in ABC rotating coordinate, which rotates at synchronous speed. The phase variation of i_d, i_q as short-lived out-of-step period would be simplified considering the relatively minor impact. In dq-axis, according to the Clark transform and Park transform, the mutual inductance M_{fd}, M_{fq}, and M_{df} of system load can be obtained as:

$$\begin{cases} M_{fd} = 1.5M_{fA} = 1.5M_{df} \\ M_{fq} = 0 \end{cases} \tag{15}$$

where M_{fA} is the maximum mutual inductance of A phase and excitation winding, which is equal to the value of B or C phase.

When EESM is in a stable state, WPT input variation state, and stator current variation state, the load excitation winding of the motor can be equivalent to a, b, and c as shown in Figure 1. Therefore, the load impedance of EESM can be expressed as:

$$Z_f = R_f + \frac{dL_f(\theta)}{d\theta}\omega_r + \frac{1}{i_f}\left(L_f(\theta)\frac{di_f}{d\theta} + M_{fd}\frac{di_d}{dt}\right) \tag{16}$$

When the stator current i_d, i_q varies according to the reference value, the excitation current i_f would fluctuate due to M_{fd}, and the voltage variation is mutual voltage. The electromagnetic torque of EESM can be obtained as:

$$T_e = \frac{3}{2}p_0\left[\left(L_q - L_d\right)i_d i_q + M_{fd} i_f i_d\right] \tag{17}$$

where p_0 is the pole pairs.

D. SRM BASED ON WPT SYSTEM

Due to the stator and rotor poles of SRM are convex, the inductance of each phase winding varies with the position of the rotor. Therefore, in order to generate continuous positive torque, the current of each phase winding should be excited based on the position of the rotor with the increased phase inductance. Set the resonant frequencies f_1, f_2, and f_3 to activate the phase A, B, C, respectively. The electromagnetic torque T_e can be expressed as:

$$T_e = \frac{1}{2}i^2\frac{dL(\theta)}{d\theta} = \frac{1}{2}i^2\frac{L_{\max} - L_{\min}}{\beta_s} \tag{18}$$

The motion equation of SRM is expressed as:

$$T_e = J\frac{d\omega_m}{dt} + B\omega_m + T_L \tag{19}$$

where i is the phase current, L is the phase inductance, L_{max} and L_{min} are the maximum and minimum phase inductance, respectively, β_s is the stator pole pitch, J is the moment inertia, B is the viscous friction coefficient, T_L is the load torque, and ω_m is the rotor speed. Assuming that all phases are identical, the voltage equation of SRM can be obtained as:

$$U = R_i + L(\theta)\frac{di}{dt} + \frac{dL(\theta)}{d\theta}i\omega_m = R_i + \frac{L_{\max} - L_{\min}}{\beta_s}i\omega_m \tag{20}$$

By combining equation with the current I_R and voltage U_R before the rectifier, the equivalent load of SRM can be obtained as follows:

$$R(\omega_m) = \frac{U_R}{I_R} = \frac{8}{\pi^2}\left(R + \frac{L_{\max} - L_{\min}}{\beta_s}\omega_m\right), \quad m = A, B, C \tag{21}$$

The resonant frequencies of the three receiving circuits of the WPT system corresponding to the three-phase SRM are different, which can be denoted as ω_{Rj} (j = 1,2,3). Then, the currents of the three receiving circuits of the WPT system can be calculated as:

$$I_{Rj}(f) = \frac{\omega M_{TRj} I_T}{\sqrt{\left(R_{Rj} + R(\omega_m)\right)^2 + \left(\omega L_{Rj} - \frac{1}{\omega C_{Rj}}\right)^2}} \tag{22}$$

III. DESIGN OF COUPLING ROTARY TRANSFORMER

The magnetic circuit model of rotary transformer is established. (see Figure. 2): the magnetic flux path (a), the magnetic resistance model (b), and electrical circuit model of its adjacent winding (c). In Figure. 2, R_c (R_{ca}, R_{cb}, and R_{cc}) represents reluctances of the magnetic flux path, R_{ag} (R_{aga} and R_{agb}) *and* R_{lk} (R_{lkp} and R_{lks}) represents reluctances of air-gap and leakage paths, respectively. L_m means the magnetizing inductance, L_{lkp} and L_{lks} represents the leakage inductance on the primary and secondary, respectively. L_m can be achieved as:

$$L_m = \frac{N_p^2}{2(R_{ca} + R_{cb} + R_{cc}) + R_{aga} + R_{agb}} \tag{23}$$

In equation (23), the reluctance of the pot core can be determined by

$$\begin{cases} R_{ca} = R_{cc} = \dfrac{\Delta z}{\mu_0\mu_r\pi(r_o^2 - r_i^2)} \\ R_{cb} = \dfrac{\ln\left(r_o/r_i\right)}{2\mu_0\mu_r\pi\,\Delta z} \end{cases} \tag{24}$$

where r_o and r_i are the outer and inner core radius of the pot core, respectively and Δz is the height of the pot core. μ_o is the permeability of free space, μ_r is the relative permeability of the material. Due to the fringing flux around the air-gap, an extra fringing flux factor F_f has been added to calculate the air-gap reluctance:

$$\begin{cases} R_{ag} = \dfrac{l_{ag}}{\mu_0\pi(r_o^2 - r_i^2)}\dfrac{1}{F_f} \\ F_f = 1 + \dfrac{l_{ag}}{\sqrt{\pi(r_o^2 - r_i^2)}}\ln\left(\dfrac{4h_{in}}{l_{ag}}\right) \end{cases} \tag{25}$$

The leakage inductance can be calculated by the energy stored in the windings:

$$\frac{1}{2}L_{lk}I^2 = \frac{1}{2}\int_v BHdv \tag{26}$$

where H represents the magnetic field strength. When the secondary winding of the rotary transformer is traversed, the

magnetic field strength in the air gap will decrease to zero. The total leakage inductance L_{lk} can be achieved based on $N_p i_p = -N_s i_s$ as:

$$L_{lk} = \mu_0 N_p^2 \frac{2\pi}{\ln\left(r_o/r_i\right)} \left(\frac{h_{wp} + h_{ws}}{3} + l_{ag} \right) \tag{27}$$

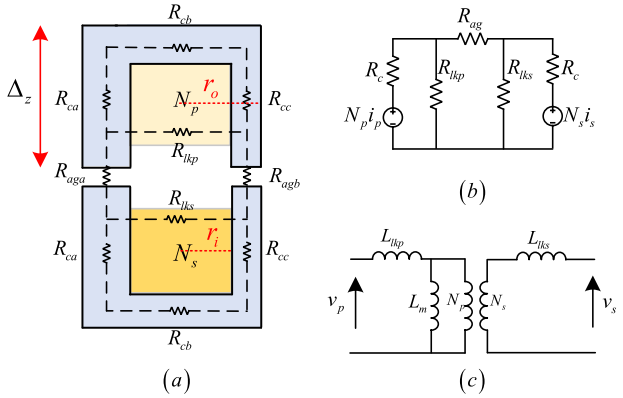

FIGURE 2. Reluctance modeling for the adjacent winding topology, (a) magnetic flux paths, (b) reluctance model, (c) equivalent electrical circuit.

A. IPT ROTARY TRANSFORMER

1) DESIGN OF MAGNETIC CORE AND WINDINGS

The magnetic core of rotary transformers has evolved from the initial two basic structures (axial pot core and radial pot core) to more new structures. For conventional axial pot core [39], [40], we can conclude several characteristics:1) Strong self-shielding properties; 2) Interchangeability due to standardized outlines; 3) Cost-effective off the shelf components. However, this type has difficulty meeting higher requirements such as high-speed applications, long-distance transmission applications, etc. The authors in [41] used fiberglass bandages to replace the ferrite material on the rotor and optimized the magnetic-core structure to adapt to high-speed applications. However, this improvement will result in higher eddy current losses in aluminum. A rotary transformer device based on local induction was proposed in [42], which only requires a portion of the magnetic core on the primary. This design needs no high-precision transformers, so it meets the requirements of high speed, safety, and low manufacturing costs. However, this improvement will lead to severe magnetic leakage and efficiency loss, so it is necessary to design resonant compensation circuits and windings, which will greatly reduce the applicability. The authors in [43] proposed a tetra polar ring coils (TPR-coils) and its decoupling method to deal with the detuning and transmission efficiency decrease of the IPT system.

All of these rotary transformers are integrated in Table 2 and Figure 5, and it can be seen from Table 2 that: 1) Although advanced radial type is more suitable for extremely high-frequency conditions, extremely-high frequency will make the mechanical strength of the transformer weaken under high-temperature and high-speed conditions. In order to balance the power transmission ability and excellent working conditions, the frequency can be maintained within 5-20 kHz. 2) The number of winding turns should be kept as small as possible to avoid prolonged power transmission processing.

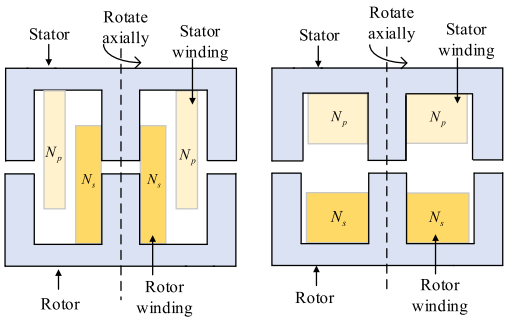

FIGURE 3. Cross-sections of winding design (a) Adjacent type (b) Coaxial type.

Adjacent type and coaxial type, two typical winding types for the axial pot core, are of great importance for rotary transformer (Figure 3). By comparing from the static state and the rotary state of the two types, it can be seen that the magnetic induction intensity on the secondary is larger than that on the primary [44]. However, the average values of the magnetic induction intensity and current density of adjacent type are larger than those of coaxial type, and coaxial type may have friction between the primary and secondary. In addition, by comparing the minimum Pareto fronts, the power loss of adjacent type is less than that of coaxial type under the same core volume. To conclude, adjacent type attracts more attention in IPT rotary transformer.

2) MATERIALS OF MAGNETIC CORE AND WINDINGS

Materials will also affect transmission performance of rotary transformer. Among these common materials (Table 3), amorphous is good at suppressing eddy currents [45], and nanocrystalline has excellent thermal stability and low loss [46]. However, the vibration and noise of amorphous increase with the increase of frequency [47], and this property will cause high loss. In addition, these two materials are fragile, which limits their large-scale use. Reversely, ferrite material is more suitable for WPT due to excellent high-frequency performance and material quality [48]. Figure 4 shows the losses and thermal stability of these materials.

In order to reduce leakage inductance, some research focused on new materials. Nonmagnetic composite materials has low rotor centrifugal stress, and it has interleaved winding, which can reduce leakage inductance [49]. This improvement will cause shaft heat up, so cooling devices are required to ensure normal operation. A new type of transformer with nanocrystalline iron core has been proposed in [50]. Through experimental comparison, it is found that this material has better magnetic permeability and lower

high-frequency loss, which can greatly improve magnetic leakage. However, due to the thin and brittle properties of nanocrystalline, the authors needed to propose specialized magnetic core structures, which increases workload.

For windings, Litz copper wire is the most common wire, and there are more and more methods for analyzing eddy current loss of this wire [51], [52]. Compared with Litz copper wire, high-temperature superconductivity (HTS) can pass very high critical current [53], however, HTS will generate significant AC loss when the frequency is between 10-100 kHz. In order to deal with this problem, P Machura et.al proposed a magnetic flux diverter to reduce the AC loss [54]. Although this method can solve the above problem, it will increase the complexity of the system. Considering the above factors, the selection of HTS should comply with the following principles: for the two-coils, the transmitter coil selects HTS and the receive coil selects copper wire; for the four-coils, the resonators selects HTS and the power coil selects copper wire [55], [56]. In addition, magnetic aluminized wire has also been used to replace Litz copper wire [57].

B. CPT ROTARY TRANSFORMER

1) DESIGN OF CPT ROTARY TRANSFORMER

The main difference between CPT and IPT is that the former replaces the inductance coils with metal plates. Compared to the inductance coils in IPT, the metal plates reduce system weight and cost, and the metal plate can be shaped to adapt to different application scenarios. Similar to the rotary transformer of IPT, the capacitor coupler of CPT is also a focus of research. In previous studies, capacitive couplers can be divided into four types: two-plates, four-plates, six-plates, and electric field repeaters. Figure 6 lists these capacitive couplers.

Among these capacitance couplers, two-plates requires fewer metal plates and can reduce cost, and single-wire type can tolerance large-misalignment applications [59], [60], [61], [62]. For four-plates with vertical position, it can increase self-capacitance [63]; for four-plates with horizontal position, it is easy to realize coupler [64]. Six-plates and electric field repeater are both composed of more coupling capacitors, so both of them has high cost. Six-plates has high coupling capacitance, and it can reduce electric field emissions [65]. Electric field repeater can provide long-distance power transmission [66]. The vertical structure of four-plates can provide a compact solution and is easy to achieve equivalent circuits, which makes it the preferred choice in CPT applications.

In addition to conventional capacitance couplers, some novel capacitance couplers with stronger functionality are gradually emerged. Separated circular capacitor coupler can avoid cross-coupling capacitance and ensure transmission efficiency [67]. The method of adding dielectric materials between the primary and secondary metal plates of CPT is used to solve the problem of weak capacitance coupling. Compared with traditional four-plates coupler, the capacitance coupling is higher and the required inductance is lower [68].

Simplifying the coupler structure while ensuring transmission performance has become a new pursuit for scholars. The author in [69] proposed a sleeve type capacitive coupler for rotational applications to improve transmission performance, and the coupler has a smaller physical size and lower resonant inductance. A hybrid coupler composed of an inductor coupler and a capacitor coupler was proposed in [70], however, the system model becomes complex due to the integration of dual parallel frameworks.

2) CPT ROTARY TRANSFORMER IN ELECTRICAL MOTORS

The application of CPT to motors can be roughly divided into three categories: synchronous motor, single/three-phase motor, and rotary. Firstly, applying CPT to synchronous motors can achieve many advantages such as arc free, speed insensitive, and maintenance free [71]. Wound field synchronous motor can select the rotary rectifier board as the coupler [72]. For single-phase motors, CPT can achieve contactless transfer between stationary and dynamic components through the capacitance of linear bearings [73]. For three-phase motors, however, the existing research is still immature, such as stacked four-plates and concentric structures found to be imbalanced [74]. Rouse et al. summarized the two three-phase CPT schemes and proposed a three-phase RCPT suitable for rotary applications [75].

For rotary applications, the author in [69] proposed a new capacitive coupled CPT system consisting of four layers of metal sleeves and two layers of dielectric. Through experimental verification, it can be seen that it has advantages such as low excitation voltage, small size, and low parameter sensitivity. In addition, some scholars selected aerodynamic fluid bearings to reduce the distance between stationary and dynamic components, then enhancing the coupling capacitance [76]. In order to improve efficiency and robustness, it is recommended to use PI control methods [77] and output feedback control methods [78] for automatic tuning circuits in rotary applications. It is recommended to use a three-phase CPT system for rotary applications to provide balance and good coupling between electrodes during the rotation process [75].

There are not many articles on capacitive coupling excitation in existing literature. Only a few research groups have established EESM working prototypes using capacitive coupling and conducted experiments under load conditions [79].

In fact, capacitive coupling has better field constraints and smaller electromagnetic interference between capacitor plates, which is superior to inductive coupling. The qualitative comparison between capacitive coupling and inductive coupling indicates that capacitive coupling may be more competitive [71]. For inductive coupling, rotating transformers inevitably require additional copper and magnetic steel, while capacitive slip rings do not. However, capacitive coupling has

TABLE 2. Rotary transformers designed for high-speed applications and EESM.

Reference	Structure	Frequency (kHz)	Input / Output	Winding turns	Air gap	Power	efficiency	Speed (rpm)
[41]	Advanced axial	18	1s2p:100V/ 9A 1p2p:222V /9A	\	\	60kW	Max：96%	10000
[39]	Axial	100	36-60V /9.72-16.2A	3-9	1mm	500-1390W	90%	\
[40]	Axial	10	-/1A	7-16	1.2mm	40W	70%	1000
[42]	Advanced radial	25.738	300V/-	70-30	1mm	\	89.8%	\
[49]	Advanced axial	20	125V/21.1A	\	2mm	10.7kW	95.9%	16000
[50]	Advanced radial	6	100V/-	\	1mm	\	\	\

TABLE 3. Features and applications of three common core materials [58].

Material	Types	Features	Applications
Ferrite	Mn-Zn, Ni-Zn	It has a very low conductivity, in which B_{sat} of Ni-Zn is smaller than that of Mn-Zn, and the conductivity of Ni-Zn is almost equal to that of insulator	Transformers, filters, chokes, MHz conditions.
Amorphous	Fe-based amorphous materials, Co-based alloys.	Co-based alloys have high permeability and low coercivity. In, addition, they have low loss at a specific frequency and magnetic flux density.	Pulse transformers, medium-frequency transformers, current transformers, etc.
Nanocrystalline	FINEMET, VITROPERM, NANOPERM, etc.	It has excellent thermal characteristic and low-loss characteristic.	EMI filters, shielding sheets, current transformers

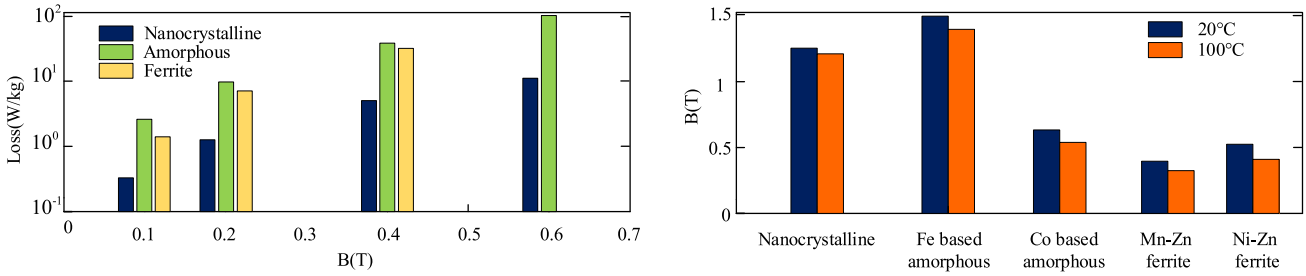

FIGURE 4. Comparison of losses and thermal behavior of different magnetic materials.

drawbacks such as low power density, complex structure, and the need for high voltage for power transmission, which not only poses a safety hazard to operators, but also generates harmful ozone () [80].

IV. COMPENSATION NETWORKS OF WPT

A. COMPENSATION NETWORKS IN IPT SYSTEM

In terms of mutual inductance and load identification, SS can accurately measure the identification result, while SP will obtain two identification results, both of which are right [81]. Besides, SS can realize constant current output, while SP does not. SS and SP are both misalignment-sensitive topologies, and this characteristic makes them unsuitable for large-misalignment applications such as electrical vehicle charging. Compared with SS and SP, PS and PP can limit instantaneous large current and prolong the service life of the capacitor. However, these two topologies have the drawbacks of high cost and high input impedance [82].

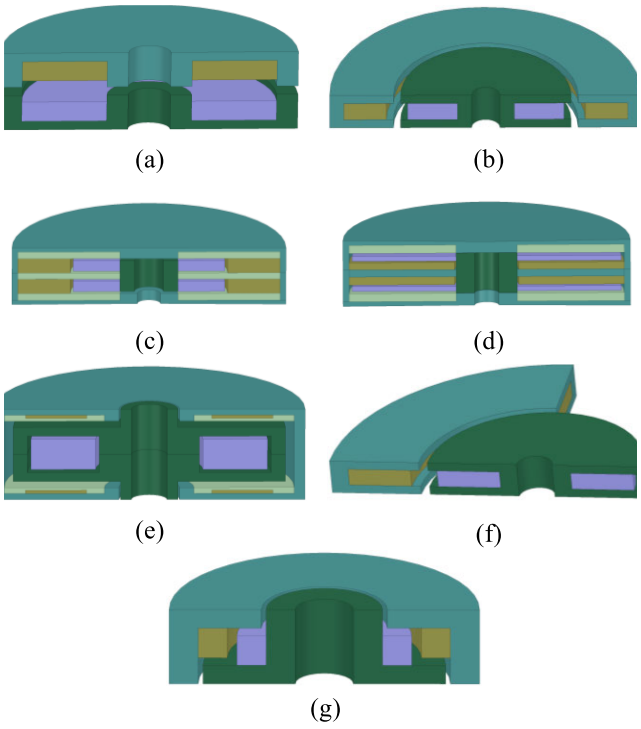

FIGURE 5. Structures of rotary transformers. (a) axial pot core [44], [47], (b) radial pot core [49], (c) type based on nanocrystalline-left-right winding structure [30], [52], (d) type based on nanocrystalline-up-down winding structure (e) double stator type [51], (f) axial type based on local induction and (g) advanced radial pot core.

High-order compensation networks have become research hotspots. S/SP can be seen as a combination of SS and SP, and research results shown that S/SP not only has the characteristics of constant voltage output (CVO), but also has high efficiency and excellent output controllability. However, this topology still has offset-sensitive characteristic, which narrow the application scope in practical projects [83], [84]. SP/S can transmit rated power under high misalignment of the receiving coil width (up to 25% in the research system) without complex control strategies and with high efficiency [85]. LCL can be used either on single-side or double-side of WPT, and the research on parameter selection of this topology has been matured [86]. In order to achieve larger constant current and higher excitation intensity, an additional capacitor and a coupling coil were added in series on LCL [87]. If the coupling coil in LCL is partially compensated by additional capacitance, LCL will evolve into LCC, and this topology can also be used for single-sided [88] or double-sided [89] applications. Although this topology requires two additional compensation capacitors, it can be independent of the load and coupling coefficient variation. All of these compensation networks are listed in Figure 7.

Considering the relative stability of rotary transformer and the characteristics of the loads connected to the WPT system, this review remarks the following compensation networks.

Firstly, SP and PP [90], [91]: both of which can be operated on the primary to control secondary current of WPT. Specifically, PP can avoid open circuit and short circuit on the secondary side, which improves the safety.

Secondly, LCL-S [92]: SS is one of the most used networks due to its simple configuration and pure resistance reflected to the primary side, however, the primary current of SS is affected by the equivalent resistance on the secondary, and this condition will cause high-coupling state, which will cause frequency-splitting phenomenon. LCL-S can suppress the frequency-splitting phenomenon due to its impedance conversion capability, and maintain simple structure simultaneously.

Thirdly, XLC/S [93]: Comparing with the previously method to suppress the power fluctuation in the primary coil, this method reduced the additional loss. Meanwhile, it can realize constant current output (CCO) and zero voltage switching (ZVS) under the flexible adjustment of the radius of the secondary coil.

For the SS type topology, the compensating capacitor is only affected by the self-inductance of the coupling coil, and the power factor reaches 1 under complete compensation conditions. Therefore, this topology enables the system to maintain stable output under dynamic changes. For SP compensation, the selection of its compensation capacitor needs to consider the changes in load and mutual inductance, and has limitations on the current amplitude at the receiving end. The PS compensation structure can still maintain high power factor and efficiency even when the coupling coefficient is small, but the value of the compensation capacitance at the transmitting end needs to consider the load. The design of PP compensation structure is complex and the power factor is low, so it has not been thoroughly studied. The output voltage of LCC-S topology will also change after mutual inductance changes, and the smaller the mutual inductance, the smaller the output voltage is only affected by mutual inductance.

B. COMPENSATION NETWORKS IN CPT SYSTEM

As the transmission distance increases, the coupling capacitance value decreases, so a suitable compensation network is inevitable. The compensation topologies of capacitive coupling have always been a focus of research. So far, scholars have proposed topologies including L, LC, LCL, LCLC, CLLC, LCCL etc. Double-L is the most typical and simple topology, which has applications in synchronous motors, three-phase motors, and rotary. However, for high-power applications, Double-L is clearly not sufficient, so double-LCL and LCLC have been proposed to increase power transmission in portable device charging applications. Experiments have shown that LCLC can achieve high power transmission through an air-gap distance of 150 mm [94]. The key aspect of LCLC is to use a large capacitor connected in parallel with the coupling capacitor to reduce the resonant inductance, however, the inductance is still larger than 200μH, which is difficult to make in practice [95]. E-LCCL topology has been proposed to deal with this difficulty [96]. In addition, some mixed topologies have also been analyzed,

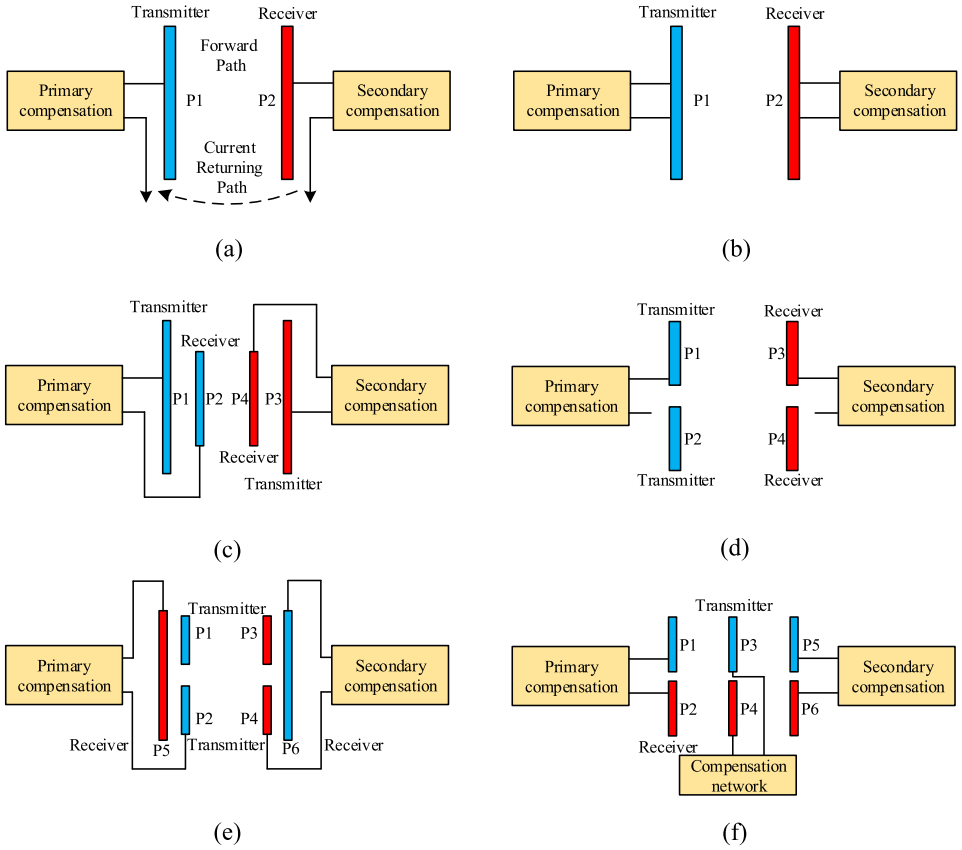

FIGURE 6. Classification of coupler structures. (a) Two-Plates, Quasi Wireless (b). Two-Plates, Single Wire (c) Four-lates, Vertical (d) Four-Plates, Horizontal (e) Six-Plates (f) Electric Field Repeater.

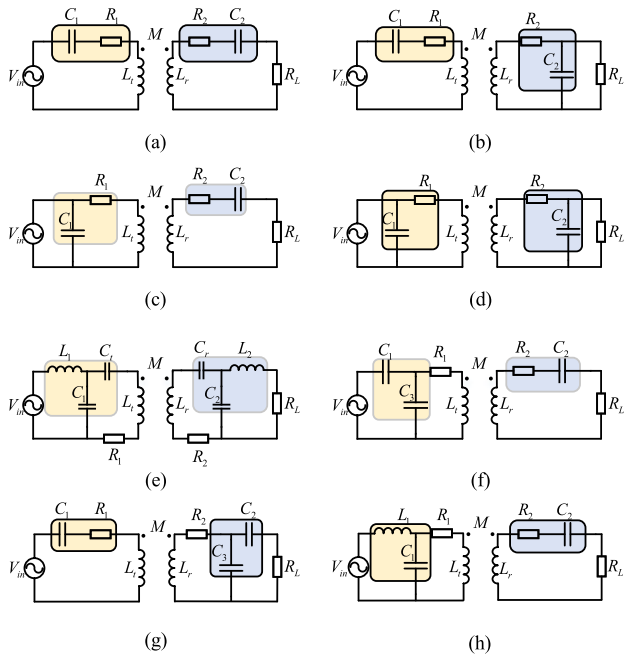

FIGURE 7. Compensation networks. (a) SS (b) SP (c) PS (d) PP (e) LCC-LCC (f) SP-S (g) S-SP (h) LCL-S.

such as LC-CLC can improve misalignment tolerance performance of couplers [97], LCL-L can reduce the number of components while maintaining good transmission performance [98]. For rotary applications, LCCL has also been proposed for rotary applications, however, complex structure results in a low applicability [99]. Table 4 lists typical compensation networks of CPT.

V. CONTROL STRATEGIES OF WPT

Maximum power transmission (MPT) and maximum efficiency transmission (MET) are two different studies on WPT. MPT studies the maximum amount of power transferred to the load, while MET focuses on the efficiency of this process. Although MPT can be achieved when the load and power supply reach a certain impedance matching, the transmission efficiency is only 50% at this time [100]. In most WPT commercial applications, constant voltage output and MET are two research hotspots, both of which are affected by load and coupling coefficient variation. How to improve transmission efficiency while ensuring constant voltage output has become a research hotspot.

A. CONSTANT VOLTAGE/CURRENT OUTPUT

There were two typical control methods for achieving constant voltage output in previous research: frequency tracking and DC-DC conversion. Among research on frequency tracking, frequency-division is a key issue related to the

transmission efficiency and capability of magnetic resonance systems. Through adjusting the frequency-division point of the inverter, the output voltage is not affected by load variation [101]. In addition, immittance networks also play a very important role in the output performance of WPT systems [102], [103].

B. MAXIMUM EFFICIENCY TRACKING

Realizing MET mainly includes the following two schemes: impedance matching and load modulation. Impedance matching usually applies for low-power charging applications with high operating frequencies (such as megahertz level). For the kHz system, impedance matching is used to change the output performance of the target, while for the MHz system, the real and imaginary parts of the load impedance change with coupling coefficient variation. The capacitor matrix contained in the impedance matching networks (IMN) is complex, and this complexity will increase significantly with the increase of power capacity, so high robustness is needed in the design process of IMN. Tunable IMN is one solution. In [104], due to coupling coefficient variation, the capacitance matrix of the primary was adjusted to the internal resistance of the voltage source, which made the system achieve MPT. According to load variation, the capacitor matrix of the secondary was adjusted to the best equivalent impedance to achieve MET. In addition, a capacitor matrix with a controllable switch can adjust continuously and has high adjustment accuracy [105], [106].

There are three types of load modulation schemes for MET control. One is to adjust the duty cycle of the dc-dc converter to maintain the equivalent load resistance at the optimal load resistance, and transmitter controller is responsible for constant voltage output [107], [108]. However, this method requires determining the mutual inductance in advance. The second scheme is to use the dc-dc converter to adjust the output voltage, while the transmitter controller searches for the minimum input power to realize MET [109], [110]. The third scheme is to add dc-dc converters on both sides of the system, and the experimental results showed that the maximum efficiency point is tracked within a wide range of coupling coefficient and load variation. However, this scheme is not suitable for most WPT systems as it completely sacrifices the simple structure of the system [111].

Overall, using DC-DC converters on the secondary can greatly avoid complex control strategies, which is at the expense of the simple structure and low cost. Therefore, more and more researchers are focusing on double-side control strategies. Li et al. proposed a collaborative control strategy of full-bridge inverter and semi-active rectifier [112]. This strategy not only avoids the DC-DC converter, but also eliminates wireless communication links between two sides, which greatly optimized the system and simplified control strategies. However, when the coupling coils exist significant misalignment, the control strategy cannot work properly, so it is necessary to optimize the system parameters. The optimization algorithm widely used in photovoltaic power generation applications is expected to improve this strategy [113]. In [112], the author proposed a collaborative control strategy of phase shift control and semi-active rectifier, and a collaborative control strategy of buck converter and semi-active rectifier was proposed in [114]. Besides, Liu et al. [115] proposed a double-sided control strategy, which achieved the same functions as [110]. The main idea of these papers is: the semi-active rectifier is used to maintain constant output current, while disturbance observation method was used to control the primary side to search for minimum input power, therefore, constant output and MET can be achieved simultaneous. Table 5 lists the comparison between double-side collaborative control and previous control strategies.

VI. FUTURE PERSPECTIVE

A. RESEARCH BOTTLENECK

1) RESONANCE

Resonance is an important factor for the system to achieve maximum transmission efficiency. Fixed resonant frequency method can simplify control methods and avoid electromagnetic interference while maintaining maximum transmission efficiency, therefore, this method achieves more extensive investigation. However, there is a lack of clear theoretical basis for the selection of compensation topology, parameter design, and control strategy [116]. To solve this problem, impedance matching network has been proposed [117], however, this improvement made it difficult to keep tuning because the secondary side can perceive the instantaneous frequency of the primary and component errors of the secondary.

2) ELECTROMAGNETIC INTERFERENCE

For electric vehicle charging and robot charging, electromagnetic interference can cause damage to the surrounding environment and human beings, and the most common electromagnetic shielding methods are aluminum shielding [122] and magnetic shielding [123]. However, aluminum or magnetic electromagnetic shielding will significantly reduce the self-inductance and mutual inductance. J Kim et.al proposed a novel reactive shielding method having shielding effectiveness (SE) and power transfer effectiveness (PTE) [124]. He et.al proposed a dual-band-coil array with novel high-order circuit compensation [125]. In future work, magnetic field research should be the priority. For robot charging, specific shielding design has also been proposed [126].

B. NOVEL APPLICATIONS

1) WIRELESS CHARGING

Wireless charging applications are mainly divided into four aspects: electric vehicle charging, robot charging, drone charging, and underwater charging. Electric vehicle charging has been a research hotspot in recent years, and the

TABLE 4. Compensation topologies of CPT.

Compensation types	Application	Coupler type	Efficiency
L-L	Three-phase motor	Electric Field Repeater[73]	95%
		Six-plates [75]	73%
	Rotary	Four-plates[76]	94%
		Six-plates[75]	73%
LC-LC	Rotary [69]	Four-plates	85.3%
LCCL-LCCL	Rotary [99]	Four-plates	76%

TABLE 5. Comparison between double-side collaborative control strategy and previous control strategies.

Reference	Distance & coupling coefficient	Maximum Efficiency (%)	Secondary circuit	Communication link
[111]	25cm & 0.04	74	Boost	Yes
[109]	10cm & 0.1	69	Buck-boost	No
[118]	5.5cm & 0.137	76	LSK	Yes
[119]	3cm & 0.09	51	Buck	Yes
[108]	5cm & 0.168	85	Buck-boost	Yes
[120]	50cm & 0.01	70	Half-bridge	No
[121]	20cm & 0.0689	73	On-off	Yes
[112]	3cm & 0.15	81	Semi-active rectifier	No
[114]	10cm & 0.25	86	Semi-active rectifier	No

design of magnetic couplers is of great importance, which is related to the issue of transmission efficiency. In recent years, many scholars have reached maturity in their research on the structure of solder pads [127]. Therefore, studying the materials of solder pads based on the structure has become a current research hotspot [128]. Future research directions should focus on new materials with low magnetic flux leakage rate and high transmission efficiency. In terms of robot charging, traditional IPT systems have been mature enough, but there is not much research on CPT systems. The challenges mainly include power transmission, system efficiency, personal safety, transmission distance, and requirements for transmission media [129]. These challenges are also common issues in electric vehicle charging, so robot charging can be seen as an application for micro-charging electric vehicles.

Drone charging and underwater charging focus more on battery life [130], [131]. In [132], the authors used blockchain technology to achieve safe and efficient revocable charging in a vehicle assisted wireless drone network. It proposed an efficient privacy protection proof scheme named PAS based on mixed state channels for revocable drone charging, where drones and UGVs act as blockchain users for off chain operations to protect privacy and efficiency, while ensuring security and fairness through on chain mechanisms. PAS consists of multi-party state channels and multiple two party state channels, responsible for fee scheduling and transaction cancellation, respectively.

For underwater charging, CPT system is the best choice due to its waterproofness. In addition, the high dielectric constant of seawater can improve the coupling capacitance [133].

2) ROTARY ULTRASONIC MACHINING

Rotary ultrasonic machining (RUM) has rotary and ultrasonic vibration characteristics, and it was used to cut hard and brittle materials such as diamond and ceramics. For RUM, the tools and working conditions will affect resonant frequency, and the machining process will affect the transducer. How to maintain good transmission performance under the changing condition has being a research hotspot. Previous studies focused on double-side compensations, Luan and Zhu studied the compensation performance of four basic compensation topologies from temperature, cutting force and ESR, and they concluded that SS compensation has the best performance [134]. Due to the tool handle occupying space, the secondary side is difficult to install compensation capacitor. Zhang proposed single-side PS dynamic compensation for the machining process, and this method can achieve higher transmission efficiency and stability [135]. However,

these studies ignore the ESR of compensation capacitor, which can cause inevitable power loss. Self-compensation theory can remedy this defect, however, this theory has poor universality [136].

Very few studies have investigated the effects of dynamic compensation with load variation on the WPT parameters, or examined WPT frequency characteristics compared with transducer frequency characteristics. From the perspective of load variations, Fu et.al proposed PS dynamic compensation and extended to the ultrasonic measurement field with WPT [137]. In future work, the authors should consider the ESRs of the compensation capacitors and the automatic control of dynamic compensation.

3) MECHANICAL ARM

Mechanical arm is widely used in conditions such as item handling, medical equipment, and excavation. The slip ring and brush on the connector of mechanical arm will cause wear and damage, so with the development of WPT, a novel mechanical arm has been designed. Atsutake Kosuge et.al proposed a rotatable transmission line coupler (RTLC), which can not only maintain a constant overlapping area at any rotation angle, but also has a strong resistance to oil and metal dust [138]. For mechanical arm, this improvement is conducive to maintaining strong anti-interference ability in intelligent logistics and other applications.

4) VEHICULAR NETWORKS

Scholars have proposed an innovative dynamic wireless information and energy transmission scheme for nano empowered vehicle networks, aimed at improving the efficiency and reliability of information and energy transmission, and providing support for future intelligent transportation and communication networks [139].

VII. CONCLUSION

This article provides a comprehensive overview of on-board wireless motors based on WPT systems.

1. The characteristics and advantages of common on-board wireless motors are comprehensively summarized and categorized according to their coupling strength.

2. Mathematical models are conducted for common wireless motors.

3. Rotary transformer is introduced to replace the ordinary coupling coil of the WPT system, thereby achieving the power transmission of three-phase on-board wireless motors. Electromagnetic models of the rotary transformer are conducted. In addition, the structures and materials of rotary transformer are summarized.

4. The resonant compensation topologies of on-board wireless motors are summarized, and the transmission characteristics of various compensation topologies are compared, which helps to select appropriate compensation topologies for different applications.

5. The control strategies of on-board wireless motors are mainly focusing on the output power and transmission efficiency. By comparing the advantages and disadvantages, these control strategies can be further improved, which can improve the transmission performance of on-board wireless motors.

6. Research difficulties and directions of on-board wireless motors are also proposed, such as electromagnetic interference and resonance, and extended this technology to other fields, including wireless charging, robotics, etc.

REFERENCES

[1] H. Jiangyi and W. Fan, "Design and testing of a small orchard tractor driven by a power battery," *Engenharia Agrícola*, vol. 43, no. 2, 2023, Art. no. e20220195.
[2] Y. Wang, B. Li, Z. Zhao, and K. Tang, "Optimal routing and charging of electric logistics vehicles based on long-distance transportation and dynamic transportation system," *Promet-Traffic Transp.*, vol. 35, no. 2, pp. 230–242, Apr. 2023.
[3] X. Sun, Z. Jin, M. Xue, and X. Tian, "Adaptive ECMS with gear shift control by grey wolf optimization algorithm and neural network for plug-in hybrid electric buses," *IEEE Trans. Ind. Electron.*, vol. 71, no. 1, pp. 667–677, Jan. 2024.
[4] X. Sun, X. Lin, D. Guo, G. Lei, and M. Yao, "Improved deadbeat predictive current control with extended state observer for dual three-phase PMSMs," *IEEE Trans. Power Electron.*, vol. 39, no. 6, pp. 6769–6782, Jun. 2024, doi: 10.1109/TPEL.2024.3370622.
[5] T. Zwerger and P. Mercorelli, "Using a bivariate polynomial in an EKF for state and inductance estimations in the presence of saturation effects to adaptively control a PMSM," *IEEE Access*, vol. 10, pp. 111545–111553, 2022.
[6] X. Sun, Y. Zhu, Y. Cai, Y. Xiong, M. Yao, and C. Yuan, "Current fault tolerance control strategy for 3-Phase switched reluctance motor combined with position signal reconstruction," *IEEE Trans. Energy Convers.*, vol. 38, no. 3, pp. 1679–1690, May 2023, doi: 10.1109/TEC.2023.3239525.
[7] A. K. Rana and A. V. Ravi Teja, "A fault-tolerant power converter with multi-switch fault diagnosis and repair capability for 4-phase 8/6 SRM drives," *IEEE Trans. Transport. Electrific.*, vol. 8, no. 3, pp. 3896–3906, Sep. 2022, doi: 10.1109/TTE.2022.3161090.
[8] Z. Shi, X. Sun, Z. Yang, Y. Cai, G. Lei, J. Zhu, and C. H. Lee, "Design optimization of a spoke type axial-flux PM machine for in-wheel drive operation," *IEEE Trans. Transport. Electrific.*, early access, Aug. 2023, doi: 10.1109/TTE.2023.3310738.
[9] M. Polat, A. Yildiz, and R. Akinci, "Performance analysis and reduction of torque ripple of axial flux permanent magnet synchronous motor manufactured for electric vehicles," *IEEE Trans. Magn.*, vol. 57, no. 7, pp. 1–9, Jul. 2021, doi: 10.1109/TMAG.2021.3078648.
[10] X. Sun, Z. Su, G. Lei, Y. Cai, and M. Yao, "Adaptive model-free predictive current control for SPMSM drives with optimal virtual vector modulation," *IEEE/ASME Trans. Mechatronics*, early access, Dec. 2023, doi: 10.1109/TMECH.2023.3332136.
[11] X. Sun, Z. Su, G. Lei, and M. Yao, "Robust predictive cascaded speed and current control for PMSM drives considering parameter variations," *IEEE Trans. Ind. Electron.*, vol. 71, no. 9, pp. 10235–10245, Dec. 2023, doi: 10.1109/TIE.2023.3337498.
[12] Y. Yu, S. Hao, S. Guo, Z. Tang, and S. Chen, "Motor torque distribution strategy for different tillage modes of agricultural electric tractors," *Agriculture*, vol. 12, no. 9, p. 1373, Sep. 2022.
[13] X. Sun, Y. Zhu, Y. Cai, M. Yao, Y. Sun, and G. Lei, "Optimized-sector-based model predictive torque control with sliding mode controller for switched reluctance motor," *IEEE Trans. Energy Convers.*, vol. 39, no. 1, pp. 379–388, Mar. 2024.
[14] S. K. Chaurasiya, A. Bhattacharya, and S. Das, "Reduced switch multilevel converter for grid fed SRM drive to improve magnetization and demagnetization characteristics of an SRM," *IEEE Trans. Ind. Appl.*, vol. 59, no. 6, pp. 6804–6816, Nov. 2023, doi: 10.1109/TIA.2023.3305594.
[15] L. Wang, J. Li, H. Nie, J. Liu, and S. Ke, "Coaxial nested couplers-based offset-tolerance rotary wireless power transfer systems for electric excitation motors," *IEEE Access*, vol. 8, pp. 44913–44923, 2020.
[16] E. Ayaz, O. Altun, and O. Keysan, "Variable carrier phase-shift method for integrated contactless field excitation system of electrically excited synchronous motors," *IEEE Trans. Power Electron.*, vol. 38, no. 10, pp. 13243–13253, Oct. 2023, doi: 10.1109/TPEL.2023.3300531.

[17] E. Ayaz, O. Altun, H. Polat, F. Karakaya, and O. Keysan, "Concurrent wireless power transfer and motor drive system with a single converter," *IEEE J. Emerg. Sel. Topics Ind. Electron.*, vol. 4, no. 1, pp. 409–418, Jan. 2023, doi: 10.1109/JESTIE.2022.3182592.
[18] C. Jiang, K. T. Chau, C. Liu, and W. Han, "Wireless DC motor drives with selectability and controllability," *Energies*, vol. 10, no. 1, p. 49, Jan. 2017, doi: 10.3390/en10010049.
[19] S. Esaki Muthu Pandara Kone, K. Yatsugi, and H. Iizuka, "Wirelessly powered motor operation in dynamic scenarios using non-hermitian parity-time symmetry," *Sci. Rep.*, vol. 13, no. 1, p. 21492, Dec. 2023, doi: 10.1038/s41598-023-47842-x.
[20] J. Jose and J. P. Therattil, "Novel L2CL–LCL topology for wireless power transmission PMSM powered electrical vehicle," *Intell. Autom. Soft Comput.*, vol. 34, no. 1, pp. 339–355, 2022, doi: 10.32604/iasc.2022.023863.
[21] Y. Huang, X. Gao, Z. Song, X. Liu, and C. Liu, "A novel wireless motor based on three-phase six-stator-winding PMSM," *IEEE Trans. Ind. Electron.*, vol. 71, no. 7, pp. 7590–7598, Jul. 2024, doi: 10.1109/TIE.2023.3301548.
[22] H. Wang, K. T. Chau, C. H. T. Lee, and X. Tian, "Design and analysis of wireless resolver for wireless switched reluctance motors," *IEEE Trans. Ind. Electron.*, vol. 70, no. 3, pp. 2221–2230, Mar. 2023, doi: 10.1109/TIE.2022.3169712.
[23] W. Han, K. T. Chau, Z. Hua, and H. Pang, "An integrated wireless motor system using laminated magnetic coupler and commutative-resonant control," *IEEE Trans. Ind. Electron.*, vol. 69, no. 5, pp. 4342–4352, May 2022.
[24] R. Manko, M. Vukotić, D. Makuc, D. Vončina, D. Miljavec, and S. Čorović, "Modelling of the electrically excited synchronous machine with the rotary transformer design influence," *Energies*, vol. 15, no. 8, p. 2832, Apr. 2022, doi: 10.3390/en15082832.
[25] J. Kang, Y. Liu, L. Sun, Z. Zhong, and M. Fu, "A reduced-order model for wirelessly excited machine based on linear approximation," *IEEE Trans. Power Electron.*, vol. 36, no. 11, pp. 12389–12399, Nov. 2021, doi: 10.1109/TPEL.2021.3079273.
[26] M. Büyük, "Wireless power transfer system with dual-frequency operation in transmitter side for motor control application," *Int. J. Circuit Theory Appl.*, vol. 51, no. 1, pp. 18–31, Jan. 2023.
[27] G. Rizzoli, M. Mengoni, A. Tani, G. Serra, L. Zarri, and D. Casadei, "Wireless power transfer using a five-phase wound-rotor induction machine for speed-controlled rotary platforms," *IEEE Trans. Ind. Electron.*, vol. 67, no. 8, pp. 6237–6247, Aug. 2020, doi: 10.1109/TIE.2019.2935988.
[28] J. Zhai, X. Zhang, S. Zhao, and Y. Zou, "Modeling and experiments of a wireless power transfer system considering scenarios from in-wheel-motor applications," *Energies*, vol. 16, no. 2, p. 739, Jan. 2023, doi: 10.3390/en16020739.
[29] N. Ali, Z. Liu, H. Armghan, and A. Armghan, "Super-twisting sliding mode controller for maximum power transfer efficiency tracking in hybrid energy storage based wireless in-wheel motor," *Sustain. Energy Technol. Assessments*, vol. 52, Aug. 2022, Art. no. 102075, doi: 10.1016/j.seta.2022.102075.
[30] C. Jiang, K. T. Chau, C. H. T. Lee, W. Han, W. Liu, and W. H. Lam, "A wireless servo motor drive with bidirectional motion capability," *IEEE Trans. Power Electron.*, vol. 34, no. 12, pp. 12001–12010, Dec. 2019, doi: 10.1109/TPEL.2019.2904757.
[31] H. Liu, Y. Mei, H. Zhou, W. Hu, Q. Deng, X. Gao, and L. Fang, "Compact and efficient wireless motor drive with bidirectional motion capability," *IEEE Trans. Power Electron.*, vol. 38, no. 12, pp. 15097–15101, Dec. 2023, doi: 10.1109/TPEL.2023.3308389.
[32] M. Sato, G. Yamamoto, D. Gunji, T. Imura, and H. Fujimoto, "Development of wireless in-wheel motor using magnetic resonance coupling," *IEEE Trans. Power Electron.*, vol. 31, no. 7, pp. 5270–5278, Jul. 2016, doi: 10.1109/TPEL.2015.2481182.
[33] J.-W. Zhang, X. Bai, W.-Y. Han, B.-H. Zhao, L.-J. Xu, and J.-J. Wei, "The design of radio frequency energy harvesting and radio frequency-based wireless power transfer system for battery-less self-sustaining applications," *Int. J. RF Microw. Comput.-Aided Eng.*, vol. 29, no. 1, Jan. 2019, Art. no. e21658.
[34] H. Ma, X. Li, B. Zhang, J. Yi, X. Wang, and J. Xu, "Design and optimization of 3-kW inductive power transfer charging system with compact asymmetric loosely coupled transformer for special applications," *Int. J. Circuit Theory Appl.*, vol. 49, no. 4, pp. 1061–1077, Apr. 2021, doi: 10.1002/cta.2909.
[35] X. Li, M. Yu, J. Zhu, W. Zheng, G. Ma, X. Deng, W. Huang, and W. A. Serdijn, "System design of a closed-loop vagus nerve stimulator comprising a wearable EEG recorder and an implantable pulse generator," *IEEE Circuits Syst. Mag.*, vol. 22, no. 3, pp. 22–40, 3rd Quart., 2022.
[36] A. I. Mahmood, S. K. Gharghan, M. A. Eldosoky, and A. M. Soliman, "Near-field wireless power transfer used in biomedical implants: A comprehensive review," *IET Power Electron.*, vol. 15, no. 16, pp. 1936–1955, Dec. 2022, doi: 10.1049/pel2.12351.
[37] K. Skarżyński and M. Słoma, "Printed electronics in radiofrequency energy harvesters and wireless power transfer rectennas for IoT applications," *Adv. Electron. Mater.*, vol. 9, no. 8, Aug. 2023, Art. no. 2300238, doi: 10.1002/aelm.202300238.
[38] M. Noohi, A. Pourmand, H. Badri Ghavifekr, and A. Mirvakili, "Design and simulation of a rectangular planar printed circuit board coil for nuclear magnetic resonance, radio frequency energy harvesting, and wireless power transfer devices," *ETRI J.*, vol. 2024, pp. 1–14, Jan. 2024, doi: 10.4218/etrij.2023-0163.
[39] J. Tang, Y. Liu, and N. Sharma, "Modeling and experimental verification of high-frequency inductive brushless exciter for electrically excited synchronous machines," *IEEE Trans. Ind. Appl.*, vol. 55, no. 5, pp. 4613–4623, Sep. 2019.
[40] M. Wardach, M. Bonislawski, R. Palka, P. Paplicki, and P. Prajzendanc, "Hybrid excited synchronous machine with wireless supply control system," *Energies*, vol. 12, no. 16, p. 3153, Aug. 2019.
[41] M. Maier and N. Parspour, "Operation of an electrical excited synchronous machine by contactless energy transfer to the rotor," *IEEE Trans. Ind. Appl.*, vol. 54, no. 4, pp. 3217–3225, Jul. 2018.
[42] Y. Luan, B. Lin, X. Ma, and X. Zhu, "Innovative contactless energy transfer accessory for rotary ultrasonic machining and its circuit compensation based on coil turns," *IEEE Trans. Ind. Electron.*, vol. 64, no. 10, pp. 7810–7818, Oct. 2017.
[43] W. Zhou, Z. Zhu, R. Mai, and Z. He, "Design and analysis of decoupled tetra-polar ring-coils for wireless power transfer in rotary mechanism applications," *IET Electr. Power Appl.*, vol. 14, no. 10, pp. 1766–1773, Oct. 2020, doi: 10.1049/iet-epa.2019.1000.
[44] Y. Yu and X. Wang, "Characteristic analysis of relatively high speed, loosely coupled rotating excitation transformers in HEV and EV drive motor excitation systems," *IEICE Electron. Exp.*, vol. 14, no. 4, 2017, Art. no. 20161218.
[45] T. Hamaguchi, R. Nakamura, K. Asano, T. Wada, and T. Suzuki, "Diffusion of boron in an amorphous iron-boron alloy," *J. Non-Crystalline Solids*, vol. 601, Feb. 2023, Art. no. 122070, doi: 10.1016/j.jnoncrysol.2022.122070.
[46] S. Singh, J. Singh, and S. K. Tripathi, "High thermopower in (00l)-oriented nanocrystalline Bi-Sb-Te thin films produced by one-step thermal evaporation process," *Vacuum*, vol. 165, pp. 12–18, Jul. 2019, doi: 10.1016/j.vacuum.2019.03.055.
[47] P. Zhang and L. Li, "Vibration and noise characteristics of high-frequency amorphous transformer under sinusoidal and non-sinusoidal voltage excitation," *Int. J. Electr. Power Energy Syst.*, vol. 123, Dec. 2020, Art. no. 106298.
[48] A. A. Ghanem and S. O. Abdellatif, "Experimentally verified numerical model for asymmetric ferrite core wireless power transfer with on-chip interfacing circuits," *E-Prime-Adv. Electr. Eng., Electron. Energy*, vol. 5, Sep. 2023, Art. no. 100262, doi: 10.1016/j.prime.2023.100262.
[49] T. Raminosoa, R. H. Wiles, and J. Wilkins, "Novel rotary transformer topology with improved power transfer capability for high-speed applications," *IEEE Trans. Ind. Appl.*, vol. 56, no. 1, pp. 277–286, Jan. 2020.
[50] C. Feng, Y. Zhang, and Q. Chi, "Design of a novel rotary transformer with accurate prediction of nanocrystalline alloy core loss using improved steinmetz formulation," *IEEE Trans. Ind. Appl.*, vol. 60, no. 2, pp. 2764–2772, Mar. 2024.
[51] S. Hiruma, Y. Otomo, and H. Igarashi, "Eddy current analysis of litz wire using homogenization-based FEM in conjunction with integral equation," *IEEE Trans. Magn.*, vol. 54, no. 3, pp. 1–4, Mar. 2018.
[52] S. Gyimóthy, S. Kaya, D. Obara, M. Shimada, M. Masuda, S. Bilicz, J. Pávó, and G. Varga, "Loss computation method for litz cables with emphasis on bundle-level skin effect," *IEEE Trans. Magn.*, vol. 55, no. 6, pp. 1–4, Jun. 2019.
[53] Z. H. Shi, X. Y. Chen, and Z. C. Qiu, "Modeling of mutual inductance between superconducting pancake coils used in wireless power transfer (WPT) systems," *IEEE Trans. Appl. Supercond.*, vol. 29, no. 2, pp. 1–4, Mar. 2019.

[54] P. Machura and Q. Li, "AC loss reduction through flux diverters for superconducting wireless charging coils at high frequencies," *IEEE Trans. Appl. Supercond.*, vol. 31, no. 3, pp. 1–10, Apr. 2021.
[55] G. Zhang, H. Yu, L. Jing, J. Li, Q. Liu, and X. Feng, "Wireless power transfer using high temperature superconducting pancake coils," *IEEE Trans. Appl. Supercond.*, vol. 24, no. 3, pp. 1–5, Jun. 2014.
[56] W. Li, T. W. Ching, C. Jiang, T. Wang, and L. Sun, "Quantitative comparison of wireless power transfer using HTS and copper coils," *IEEE Trans. Appl. Supercond.*, vol. 29, no. 5, pp. 1–6, Aug. 2019.
[57] Y. Bu, S. Endo, and T. Mizuno, "Improvement in the transmission efficiency of EV wireless power transfer system using a magnetoplated aluminum pipe," *IEEE Trans. Magn.*, vol. 54, no. 11, pp. 1–5, Nov. 2018.
[58] D. Rodriguez-Sotelo, M. A. Rodriguez-Licea, A. G. Soriano-Sanchez, A. Espinosa-Calderon, and F. J. Perez-Pinal, "Advanced ferromagnetic materials in power electronic converters: A state of the art," *IEEE Access*, vol. 8, pp. 56238–56252, 2020.
[59] F. Lu, H. Zhang, and C. Mi, "A two-plate capacitive wireless power transfer system for electric vehicle charging applications," *IEEE Trans. Power Electron.*, vol. 33, no. 2, pp. 964–969, Feb. 2018.
[60] B. Luo, T. Long, R. Mai, R. Dai, Z. He, and W. Li, "Analysis and design of hybrid inductive and capacitive wireless power transfer for high-power applications," *IET Power Electron.*, vol. 11, no. 14, pp. 2263–2270, Nov. 2018, doi: 10.1049/iet-pel.2018.5279.
[61] K. Yi, "Capacitive coupling wireless power transfer with quasi-LLC resonant converter using electric vehicles' windows," *Electronics*, vol. 9, no. 4, p. 676, Apr. 2020, doi: 10.3390/electronics9040676.
[62] B. Minnaert and G. Monti, "Optimization of a capacitive wireless power transfer system with two electric field repeaters," *Int. J. Circuit Theory Appl.*, vol. 51, no. 6, pp. 2623–2637, Jun. 2023, doi: 10.1002/cta.3564.
[63] H. Zhang, F. Lu, H. Hofmann, W. Liu, and C. C. Mi, "A four-plate compact capacitive coupler design and LCL-compensated topology for capacitive power transfer in electric vehicle charging application," *IEEE Trans. Power Electron.*, vol. 31, no. 12, pp. 8541–8551, Dec. 2016.
[64] Q. Zhu, L. J. Zou, M. Su, and A. P. Hu, "Four-plate capacitive power transfer system with different grounding connections," *Int. J. Electr. Power Energy Syst.*, vol. 115, Feb. 2020, Art. no. 105494, doi: 10.1016/j.ijepes.2019.105494.
[65] H. Zhang, F. Lu, H. Hofmann, W. Liu, and C. C. Mi, "Six-plate capacitive coupler to reduce electric field emission in large air-gap capacitive power transfer," *IEEE Trans. Power Electron.*, vol. 33, no. 1, pp. 665–675, Jan. 2018.
[66] H. Zhang, F. Lu, H. Hofmann, W. Liu, and C. C. Mi, "An LC-compensated electric field repeater for long-distance capacitive power transfer," *IEEE Trans. Ind. Appl.*, vol. 53, no. 5, pp. 4914–4922, Sep. 2017.
[67] C. Park, J. Park, Y. Shin, J. Kim, S. Huh, D. Kim, S. Park, and S. Ahn, "Separated circular capacitive coupler for reducing cross-coupling capacitance in drone wireless power transfer system," *IEEE Trans. Microw. Theory Techn.*, vol. 68, no. 9, pp. 3978–3985, Sep. 2020.
[68] M. Z. Erel, K. C. Bayindir, and M. T. Aydemir, "A new capacitive coupler design for wireless capacitive power transfer applications," *Eng. Sci. Technol., Int. J.*, vol. 40, Apr. 2023, Art. no. 101364, doi: 10.1016/j.jestch.2023.101364.
[69] X.-Y. Wu, Y.-G. Su, A. P. Hu, L. J. Zou, and Z. Liu, "A sleeve-type capacitive power transfer system with different coupling arrangements for rotary application," *IEEE Access*, vol. 8, pp. 69148–69159, 2020.
[70] X. Gao, C. Liu, H. Zhou, W. Hu, Y. Huang, Y. Xiao, Z. Lei, and J. Chen, "Design and analysis of a new hybrid wireless power transfer system with a space-saving coupler structure," *IEEE Trans. Power Electron.*, vol. 36, no. 5, pp. 5069–5081, May 2021.
[71] D. C. Ludois, J. K. Reed, and K. Hanson, "Capacitive power transfer for rotor field current in synchronous machines," *IEEE Trans. Power Electron.*, vol. 27, no. 11, pp. 4638–4645, Nov. 2012.
[72] S. Hagen, M. Tisler, J. Dai, I. P. Brown, and D. C. Ludois, "Use of the rotating rectifier board as a capacitive power coupler for brushless wound field synchronous machines," *IEEE J. Emerg. Sel. Topics Power Electron.*, vol. 10, no. 1, pp. 170–183, Feb. 2022.
[73] J. Dai, S. S. Hagen, and D. C. Ludois, "High-efficiency multiphase capacitive power transfer in sliding carriages with closed-loop burst-mode current control," *IEEE J. Emerg. Sel. Topics Power Electron.*, vol. 7, no. 2, pp. 1388–1398, Jun. 2019.
[74] Y.-G. Su, Y.-M. Zhao, A. P. Hu, Z.-H. Wang, C.-S. Tang, and Y. Sun, "An F-type compensated capacitive power transfer system allowing for sudden change of pickup," *IEEE J. Emerg. Sel. Topics Power Electron.*, vol. 7, no. 2, pp. 1084–1093, Jun. 2019.
[75] C. D. Rouse, S. R. Cove, Y. Salami, P. Arsenault, and A. Bartlett, "Three-phase resonant capacitive power transfer for rotary applications," *IEEE J. Emerg. Sel. Topics Power Electron.*, vol. 10, no. 1, pp. 160–169, Feb. 2022.
[76] D. C. Ludois, M. J. Erickson, and J. K. Reed, "Aerodynamic fluid bearings for translational and rotating capacitors in noncontact capacitive power transfer systems," *IEEE Trans. Ind. Appl.*, vol. 50, no. 2, pp. 1025–1033, Mar. 2014.
[77] N. Nabila, S. Saat, Y. Yusop, M. S. M. Isa, and A. A. Basari, "The design of auto-tuning capacitive power transfer for rotary applications using phased-locked-loop," *Int. J. Power Electron. Drive Syst. (IJPEDS)*, vol. 10, no. 1, p. 307, Mar. 2019.
[78] S. Zang, K. Lu, S. K. Nguang, and W. Sun, "Robust H_∞ output feedback control of a rotary capacitive power transfer system," *IEEE Access*, vol. 7, pp. 113452–113462, 2019.
[79] A. Di Gioia, I. P. Brown, Y. Nie, R. Knippel, D. C. Ludois, J. Dai, S. Hagen, and C. Alteheld, "Design and demonstration of a wound field synchronous machine for electric vehicle traction with brushless capacitive field excitation," *IEEE Trans. Ind. Appl.*, vol. 54, no. 2, pp. 1390–1403, Mar. 2018.
[80] M. Biswal, P. Sharma, N. Shete, S. Sokande, and P. Tayade, "Study and survey of wireless charging technologies," *Int. J. Adv. Res. Comput. Eng. Technol.*, vol. 5, no. 5, pp. 1450–1453, 2016.
[81] J. Yin, D. Lin, T. Parisini, and S. Y. Hui, "Front-end monitoring of the mutual inductance and load resistance in a series–series compensated wireless power transfer system," *IEEE Trans. Power Electron.*, vol. 31, no. 10, pp. 7339–7352, Oct. 2016.
[82] J. Sallan, J. L. Villa, A. Llombart, and J. F. Sanz, "Optimal design of ICPT systems applied to electric vehicle battery charge," *IEEE Trans. Ind. Electron.*, vol. 56, no. 6, pp. 2140–2149, Jun. 2009.
[83] J. Hou, Q. Chen, X. Ren, X. Ruan, S.-C. Wong, and C. K. Tse, "Precise characteristics analysis of series/series–parallel compensated contactless resonant converter," *IEEE J. Emerg. Sel. Topics Power Electron.*, vol. 3, no. 1, pp. 101–110, Mar. 2015.
[84] Y. Yao, Y. Wang, X. Liu, K. Lu, and D. Xu, "Analysis and design of an S/SP compensated IPT system to minimize output voltage fluctuation versus coupling coefficient and load variation," *IEEE Trans. Veh. Technol.*, vol. 67, no. 10, pp. 9262–9272, Oct. 2018.
[85] J. L. Villa, J. Sallan, J. F. Sanz Osorio, and A. Llombart, "High-misalignment tolerant compensation topology for ICPT systems," *IEEE Trans. Ind. Electron.*, vol. 59, no. 2, pp. 945–951, Feb. 2012.
[86] J. Hou, Q. Chen, S.-C. Wong, C. K. Tse, and X. Ruan, "Analysis and control of series/series–parallel compensated resonant converter for contactless power transfer," *IEEE J. Emerg. Sel. Topics Power Electron.*, vol. 3, no. 1, pp. 124–136, Mar. 2015.
[87] H. Hao, G. A. Covic, and J. T. Boys, "An approximate dynamic model of LCL-*T*-based inductive power transfer power supplies," *IEEE Trans. Power Electron.*, vol. 29, no. 10, pp. 5554–5567, Oct. 2014.
[88] Z. Yuan, M. Saeedifard, C. Cai, Q. Yang, P. Zhang, and H. Lin, "A misalignment tolerant design for a dual-coupled LCC-S-compensated WPT system with load-independent CC output," *IEEE Trans. Power Electron.*, vol. 37, no. 6, pp. 7480–7492, Jun. 2022.
[89] S. Li, W. Li, J. Deng, T. D. Nguyen, and C. C. Mi, "A double-sided LCC compensation network and its tuning method for wireless power transfer," *IEEE Trans. Veh. Technol.*, vol. 64, no. 6, pp. 2261–2273, Jun. 2015.
[90] M. Ishihara, K. Umetani, H. Umegami, E. Hiraki, and M. Yamamoto, "Quasi-duality between SS and SP topologies of basic electric-field coupling wireless power transfer system," *Electron. Lett.*, vol. 52, no. 25, pp. 2057–2059, Dec. 2016.
[91] X. Shu, G. Wu, and Y. Jiang, "Comparative analysis of SS, SP, PP and PS topologies for magnetic coupled wireless power transfer system composed of the negative resistor," *Energies*, vol. 16, no. 21, p. 7336, Oct. 2023, doi: 10.3390/en16217336.
[92] Y. Hou, S. Sun, Z. Liu, X. Wei, S. Qiao, G. Feng, and B. Zhang, "Wireless power transfer system based on LCC/LCL-S variable structure with constant output power," *Energy Rep.*, vol. 8, pp. 850–862, Jul. 2022, doi: 10.1016/j.egyr.2022.02.033.

[93] T. Li, Y. Wang, Z. Lang, C. Qi, X. Jin, X. Chen, and D. Xu, "Analysis and design of rotary wireless power transfer system with dual-coupled XLC/S compensation topology," *IEEE Trans. Ind. Appl.*, vol. 59, no. 2, pp. 2639–2649, Mar. 2023.
[94] L. Yi and J. Moon, "Double-sided LC-compensated capacitive wireless power transfer system with admittance-based matching networks," *J. Power Electron.*, vol. 24, no. 4, pp. 652–661, Apr. 2024, doi: 10.1007/s43236-023-00742-9.
[95] F. Lu, H. Zhang, H. Hofmann, and C. Mi, "A double-sided LCLC-compensated capacitive power transfer system for electric vehicle charging," *IEEE Trans. Power Electron.*, vol. 30, no. 11, pp. 6011–6014, Nov. 2015.
[96] K. K. Hasan, S. Saat, Y. Yusop, M. A. Majid, and M. S. Ramli, "Analysis and design of class E-LCCL compensation circuit topology circuit topology for capacitive power transfer system," *Int. J. Power Electron. Drive Syst. (IJPEDS)*, vol. 12, no. 2, p. 1265, Jun. 2021.
[97] B. Luo, R. Mai, L. Guo, D. Wu, and Z. He, "LC–CLC compensation topology for capacitive power transfer system to improve misalignment performance," *IET Power Electron.*, vol. 12, no. 10, pp. 2626–2633, Aug. 2019.
[98] X. Wu, Y. Su, X. Hou, X. Qing, and X. Dai, "Study on load adaptation of capacitive power transfer system with a four-plate compact capacitive coupler," *Electr. Eng.*, vol. 101, no. 3, pp. 733–742, Sep. 2019.
[99] Y. Yusop, S. Saat, Z. Ghani, H. Husin, and S. K. Nguang, "Cascaded boost-class-E for rotary capacitive power transfer system," *J. Eng.*, vol. 2019, no. 17, pp. 3742–3748, Jun. 2019.
[100] S. Y. R. Hui, W. Zhong, and C. K. Lee, "A critical review of recent progress in mid-range wireless power transfer," *IEEE Trans. Power Electron.*, vol. 29, no. 9, pp. 4500–4511, Sep. 2014.
[101] W.-Q. Niu, J.-X. Chu, W. Gu, and A.-D. Shen, "Exact analysis of frequency splitting phenomena of contactless power transfer systems," *IEEE Trans. Circuits Syst. I, Reg. Papers*, vol. 60, no. 6, pp. 1670–1677, Jun. 2013.
[102] Z. Huang, T. Qin, X. L. Li, L. Ding, H. H.-C. Iu, and C. K. Tse, "Synthesis of inductive power transfer converters with dual immittance networks for inherent CC-to-CV charging profiles," *IEEE Trans. Power Electron.*, vol. 39, no. 6, pp. 7766–7777, Jun. 2024, doi: 10.1109/TPEL.2024.3382112.
[103] A. Z. Khan, K. H. Loo, and Y. M. Lai, "Design, analysis, and performance characterization of dual-active-bridge DC–DC converter utilizing three-phase resonant immittance network," *IEEE Trans. Power Electron.*, vol. 34, no. 2, pp. 1159–1180, Feb. 2019, doi: 10.1109/TPEL.2018.2833744.
[104] K. Zhang, W. Gao, R. Shi, Z. Yan, B. Song, and A. P. Hu, "An impedance matching network tuning method for constant current output under mutual inductance and load variation of IPT system," *IEEE Trans. Power Electron.*, vol. 35, no. 10, pp. 11108–11118, Oct. 2020.
[105] H. Shui, D. Yu, S. Yu, H. H. C. Iu, T. Fernando, and H. Cheng, "An autonomous impedance adaptation strategy for wireless power transfer system using phase-controlled switched capacitors," *IEEE J. Emerg. Sel. Topics Power Electron.*, vol. 9, no. 2, pp. 2303–2316, Apr. 2021.
[106] J. Kim, D.-H. Kim, and Y.-J. Park, "Free-positioning wireless power transfer to multiple devices using a planar transmitting coil and switchable impedance matching networks," *IEEE Trans. Microw. Theory Techn.*, vol. 64, no. 11, pp. 3714–3722, Nov. 2016.
[107] M. Fu, C. Ma, and X. Zhu, "A cascaded boost–buck converter for high-efficiency wireless power transfer systems," *IEEE Trans. Ind. Informat.*, vol. 10, no. 3, pp. 1972–1980, Aug. 2014.
[108] X. Dai, X. Li, Y. Li, and A. P. Hu, "Maximum efficiency tracking for wireless power transfer systems with dynamic coupling coefficient estimation," *IEEE Trans. Power Electron.*, vol. 33, no. 6, pp. 5005–5015, Jun. 2018.
[109] W. X. Zhong and S. Y. R. Hui, "Maximum energy efficiency tracking for wireless power transfer systems," *IEEE Trans. Power Electron.*, vol. 30, no. 7, pp. 4025–4034, Jul. 2015.
[110] Y. Yang, W. Zhong, S. Kiratipongvoot, S.-C. Tan, and S. Y. R. Hui, "Dynamic improvement of series–series compensated wireless power transfer systems using discrete sliding mode control," *IEEE Trans. Power Electron.*, vol. 33, no. 7, pp. 6351–6360, Jul. 2018.
[111] H. Li, J. Li, K. Wang, W. Chen, and X. Yang, "A maximum efficiency point tracking control scheme for wireless power transfer systems using magnetic resonant coupling," *IEEE Trans. Power Electron.*, vol. 30, no. 7, pp. 3998–4008, Jul. 2015.
[112] Z. Li, K. Song, J. Jiang, and C. Zhu, "Constant current charging and maximum efficiency tracking control scheme for supercapacitor wireless charging," *IEEE Trans. Power Electron.*, vol. 33, no. 10, pp. 9088–9100, Oct. 2018.
[113] M. Boztepe, F. Guinjoan, G. Velasco-Quesada, S. Silvestre, A. Chouder, and E. Karatepe, "Global MPPT scheme for photovoltaic string inverters based on restricted voltage window search algorithm," *IEEE Trans. Ind. Electron.*, vol. 61, no. 7, pp. 3302–3312, Jul. 2014.
[114] K. Song, R. Wei, G. Yang, H. Zhang, Z. Li, X. Huang, J. Jiang, C. Zhu, and Z. Du, "Constant current charging and maximum system efficiency tracking for wireless charging systems employing dual-side control," *IEEE Trans. Ind. Appl.*, vol. 56, no. 1, pp. 622–634, Jan. 2020.
[115] X. Liu, T. Wang, X. Yang, and H. Tang, "Analysis of efficiency improvement in wireless power transfer system," *IET Power Electron.*, vol. 11, no. 2, pp. 302–309, Feb. 2018.
[116] J. Zhang, J. Zhao, Y. Zhang, and F. Deng, "A wireless power transfer system with dual switch-controlled capacitors for efficiency optimization," *IEEE Trans. Power Electron.*, vol. 35, no. 6, pp. 6091–6101, Jun. 2020.
[117] D.-H. Kim and D. Ahn, "Self-tuning LCC inverter using PWM-controlled switched capacitor for inductive wireless power transfer," *IEEE Trans. Ind. Electron.*, vol. 66, no. 5, pp. 3983–3992, May 2019.
[118] D. Ahn, S. Kim, J. Moon, and I.-K. Cho, "Wireless power transfer with automatic feedback control of load resistance transformation," *IEEE Trans. Power Electron.*, vol. 31, no. 11, pp. 7876–7886, Nov. 2016.
[119] T.-D. Yeo, D. Kwon, S.-T. Khang, and J.-W. Yu, "Design of maximum efficiency tracking control scheme for closed-loop wireless power charging system employing series resonant tank," *IEEE Trans. Power Electron.*, vol. 32, no. 1, pp. 471–478, Jan. 2017.
[120] H. Li, J. Fang, S. Chen, K. Wang, and Y. Tang, "Pulse density modulation for maximum efficiency point tracking of wireless power transfer systems," *IEEE Trans. Power Electron.*, vol. 33, no. 6, pp. 5492–5501, Jun. 2018.
[121] W. Zhong and S. Y. R. Hui, "Maximum energy efficiency operation of series–series resonant wireless power transfer systems using on-off keying modulation," *IEEE Trans. Power Electron.*, vol. 33, no. 4, pp. 3595–3603, Apr. 2018.
[122] J. Li, F. Yin, and L. Wang, "Transmission efficiency of different shielding structures in wireless power transfer systems for electric vehicles," *CSEE J. Power Energy Syst.*, vol. 7, no. 6, pp. 1247–1255, Nov. 2021.
[123] M. Mohammad, O. C. Onar, V. P. Galigekere, G.-J. Su, and J. Wilkins, "Magnetic shield design for the double-D coil-based wireless charging system," *IEEE Trans. Power Electron.*, vol. 37, no. 12, pp. 15740–15752, Dec. 2022.
[124] J. Kim and S. Ahn, "Dual loop reactive shield application of wireless power transfer system for leakage magnetic field reduction and efficiency enhancement," *IEEE Access*, vol. 9, pp. 118307–118323, 2021.
[125] X. He, Y. Zeng, R. Liu, C. Lu, C. Rong, and M. Liu, "A dual-band coil array with novel high-order circuit compensation for shielding design in EV wireless charging system," *IEEE Trans. Ind. Electron.*, vol. 71, no. 3, pp. 2545–2555, Mar. 2024, doi: 10.1109/TIE.2023.3266567.
[126] E. K. Hamza, K. D. Salman, and S. N. Jaafar, "Wireless sensor network for robot navigation," in *Mobile Robot: Motion Control and Path Planning*, A. T. Azar, I. K. Ibraheem, and A. J. Humaidi, Eds. Cham, Switzerland: Springer, 2023, pp. 643–670.
[127] F. Y. Lin, G. A. Covic, and J. T. Boys, "Evaluation of magnetic pad sizes and topologies for electric vehicle charging," *IEEE Trans. Power Electron.*, vol. 30, no. 11, pp. 6391–6407, Nov. 2015.
[128] B. S. Gu, T. Dharmakeerthi, S. Kim, M. J. O'Sullivan, and G. A. Covic, "Optimized magnetic core layer in inductive power transfer pad for electric vehicle charging," *IEEE Trans. Power Electron.*, vol. 38, no. 10, pp. 11964–11973, Oct. 2023, doi: 10.1109/TPEL.2023.3299959.
[129] W. C. Cheah, S. A. Watson, and B. Lennox, "Limitations of wireless power transfer technologies for mobile robots," *Wireless Power Transf.*, vol. 6, no. 2, pp. 175–189, Sep. 2019.
[130] C. Rong et al., "Coupling mechanism optimization to improve misalignment tolerance in UAV wireless charging systems," *J. Power Electron.*, pp. 1–15, May 2024, doi: 10.1007/s43236-024-00839-9.
[131] M. Lin, F. Zhang, C. Yang, D. Li, and R. Lin, "Design of bidirectional power converters coupled with coils for wireless charging of AUV docking systems," *J. Mar. Sci. Technol.*, vol. 27, no. 2, pp. 873–886, Mar. 2022, doi: 10.1007/s00773-022-00877-7.
[132] X. Jia, X. Song, and C. Yu, "Privacy-preserving attestation scheme for revocable UAV charging using hybrid state channels," *Electronics*, vol. 12, no. 19, p. 3998, Sep. 2023.

[133] H. Zhang and F. Lu, "Insulated coupler structure design for the long-distance freshwater capacitive power transfer," *IEEE Trans. Ind. Informat.*, vol. 16, no. 8, pp. 5191–5201, Aug. 2020.
[134] Y. Luan, B. Lin, Q. Yang, and J. Duan, "Effect of temperature and radial force on the transmission performance of contactless power transfer for rotary ultrasonic grinding," *IET Electr. Power Appl.*, vol. 11, no. 7, pp. 1169–1176, Aug. 2017.
[135] J. Zhang, Z. Long, C. Wang, F. Ren, and Y. Li, "Novel optimization approach in ultrasonic machining: Unilateral compensation for resonant vibration in primary side," *IEEE Access*, vol. 7, pp. 34131–34140, 2019.
[136] X. Jiang, K. Wang, R. Shao, J. K. Mills, and D. Zhang, "Self-compensation theory and design of contactless energy transfer and vibration system for rotary ultrasonic machining," *IEEE Trans. Power Electron.*, vol. 33, no. 10, pp. 8650–8660, Oct. 2018.
[137] Y. Fu and A. Wang, "Dynamic compensation optimization and frequency characteristic analysis for contactless energy transfer under load variations in rotary ultrasonic machining," *IEEE Trans. Ind. Electron.*, vol. 70, no. 3, pp. 2948–2958, Mar. 2023.
[138] A. Kosuge, M. Hamada, and T. Kuroda, "A 6-Gb/s inductively-powered non-contact connector with rotatable transmission line coupler and interface bridge IC," *IEEE J. Solid-State Circuits*, vol. 57, no. 2, pp. 535–545, Feb. 2022.
[139] L. Feng, A. Ali, M. Iqbal, F. Ali, I. Raza, M. H. Siddiqi, M. Shafiq, and S. A. Hussain, "Dynamic wireless information and power transfer scheme for nano-empowered vehicular networks," *IEEE Trans. Intell. Transp. Syst.*, vol. 22, no. 7, pp. 4088–4099, Jul. 2021.

KE LI received the B.S. degree in automation, the M.S. degree in power electronics and power transmission, and the Ph.D. degree in control engineering from Jiangsu University, Zhenjiang, China, in 2005, 2008, and 2019, respectively.

Since 2005, she has been with Jiangsu University, where she is currently an Associate Professor with the School of Electrical and Information Engineering. Her research interests include wireless power transfer, motor control, hybrid electric vehicles, and intelligent control.

YUANMENG LIU was born in Xuzhou, Jiangsu, China, in 1997. He received the B.S. degree in engineering from Yancheng Institute of Technology, Yancheng, China, in 2021. He is currently pursuing the M.E. degree with the School of Electrical and Information Engineering, Jiangsu University, Zhenjiang.

His current research interests include wireless power transfer system control strategy and particle swarm optimization (PSO).

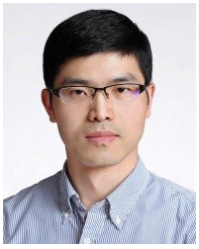

XIAODONG SUN (Senior Member, IEEE) received the B.Sc. degree in electrical engineering and the M.Sc. and Ph.D. degrees in control engineering from Jiangsu University, Zhenjiang, China, in 2004, 2008, and 2011, respectively.

Since 2004, he has been with Jiangsu University, where he is currently a Professor of vehicle engineering with the Automotive Engineering Research Institute. From 2014 to 2015, he was a Visiting Professor with the School of Electrical, Mechanical, and Mechatronic Systems, University of Technology Sydney, Sydney, Australia. His current research interests include electrified vehicles, electrical machines, electrical drives, and energy management. He is the author or coauthor of more than 100 refereed technical articles and one book and is the holder of 42 patents in his areas of interest. He is an Associate Editor of IEEE TRANSACTIONS ON INDUSTRIAL ELECTRONICS and IEEE TRANSACTIONS ON TRANSPORTATION ELECTRIFICATION and an Editor of IEEE TRANSACTIONS ON ENERGY CONVERSION.

XIANG TIAN was born in Zhenjiang, Jiangsu, China, in 1983. He received the B.S. degree in electrical engineering, the M.S. degree in power electronics and power transmission, and the Ph.D. degree in vehicle engineering from Jiangsu University, Zhenjiang, in 2006, 2009, and 2018, respectively.

He is currently a Lecturer with the Automotive Engineering Research Institute, Jiangsu University. His current research interests include electric vehicles, hybrid electric vehicles, parameter matching, optimal energy control strategy, and vehicle powertrain control.

GANG LEI (Senior Member, IEEE) received the B.S. degree in mathematics from Huanggang Normal University, China, in 2003, and the M.S. degree in mathematics and Ph.D. degree in electrical engineering from Huazhong University of Science and Technology, China, in 2006 and 2009, respectively.

He is currently a Senior Lecturer with the School of Electrical and Data Engineering, University of Technology Sydney (UTS), Australia. His research interests include computational electromagnetics, design optimization and control of electrical drive systems, and renewable energy systems. He is an Associate Editor of IEEE TRANSACTIONS ON INDUSTRIAL ELECTRONICS and IEEE TRANSACTIONS ON TRANSPORTATION ELECTRIFICATION and an Editor of IEEE TRANSACTIONS ON ENERGY CONVERSION.